Improvement of Regenerative Pump Performance by Using Blade with Combined Angles Modification

Ahmed Tahoun [a,*], Abouelmagd Abelsamie[b], A.A.Hafiz[a]

[a]Laboratory of Turbomachinery, Faculty of Engineering (Elmataria), Helwan University, Cairo, Egypt
[b]Laboratory of Fluid Mechanics, Faculty of Engineering (Elmataria), Helwan University, Cairo, Egypt

Abstract

Regenerative pumps (RP) are one of the rotor-dynamic machine types that can develop high pressure head with a single impeller at low flowrates. Researchers and manufacturers are driven to investigate the improvement of the head of the pump improvement using a various type of modifications, as the head of pump is one of the main effective parameters which indicates the performance of any operating pump. These regenerative pumps are used in many fields of applications such as chemical, micro, bio, micro heat exchangers, etc. Therefore, a lot of researches examined the effect of different possible design modifications on the head of the RP. Changing one of the angles of the blades (inclination or chevron angles) was found to have a significant impact on the performance of the pump compared to the standard pump with zero angles blade. This present research provides an eminent head enhancement for the RP by using a suitable combination of blade angles modification. This enhancement is obtained numerically using ANSYS-CFX 19.1 software, after validating the new model by comparing the simulation results with the available published experimental ones. The suggested modification applied is the double forward impeller, DFB, with chevron angle α=+15^o and inclination angle β=+15^o. An increase in the performance of this type of pumps at the tested conditions by 40 % in head is acquired compared with that of the standard pump.

Keywords: Regenerative Pump (RP), Pump Performance, Chevron Blade Angle, Inclination Blade Angle

Nomenclatures

A_c	Area in the casing flow path [m^2]
A_p	Pipe cross-section area [m^2]
a_1	Depth of the casing flow path [m]
a_2	Radial width of the casing flow path [m]
b_1	Depth of the vane channel [m]
b_2	Radial width of the vane channel [m]
c_1	Axial clearance between the impeller and the casing [m]
c_2	Radial clearance between the impeller and the casing [m]
D_1	Inner diameter of the casing flow path [m]
D_T	Diameter of the impeller [m]
g	Gravitational acceleration [m/s^2]
N	Number of the mesh elements [-]
P_d	Pressure at the outlet pipe tape [Pa]
P_s	Pressure at the inlet pipe tape [Pa]
ΔP	Pressure difference [Pa], $\Delta P = (P_d - P_s)$
Q	Volume flow rate [m^3/s]
T	Torque [Nm.]
t_1	Thickness of vane [m]
U_T	Tip velocity of the impeller [m/s]
X, Y and Z	Axial coordinate [m]

Greek letters

α	Inlet blade angle (Chevron angle) [degree]
β	Outlet blade angle (Inclination angle) [degree]
ρ	Density [kg/m^3]
τ	Torque coefficient [-]
ω	Rotational speed [rpm]
η	Efficiency [-]
Ψ	Pressure coefficient [-]
$\emptyset$	Flow coefficient [-]

Abbreviations

DFB	Double Forward Blades
RB	Radial Impeller Blades
RP	Regenerative Pumps
SFC	Single Forward Chevron Blades
SFI	Single Forward Inclination Blades

1- Introduction

Pumps are divided into two main families; each has its own purposes and applications. These two families are namely, the positive displacement and the dynamic pumps. The regenerative pumps (RP) are belonging to the dynamic pumps category. They have many commercial and scientific names such as regenerative pump, peripheral pump, side-flow channel pump, and turbine pump. This type of pump is used where high discharged heads are required with a small volume flow rate. Fortunately, this pump shares some of the characteristics of the positive displacement pumps without any wear or lubrication problems and also has a low specific speed. In the two-phase flow applications, comparing with other centrifugal pumps, RP are capable of handling large gas or vapor proportions without any interruption in liquid stream with excellent self-priming, also no cavitation is found. Due to centrifugal forces, the fluid in the RP flows inside a peripheral flow channel spirally and re-enters the peripheral path of blades several times starting from the inlet port and ended with the outlet port as shown in Fig. 1. Furthermore, because of the repetitive treatment on the fluid by the blades of the impeller, RP generates a head equivalent to that of several stages of centrifugal impeller with comparable tip speeds.

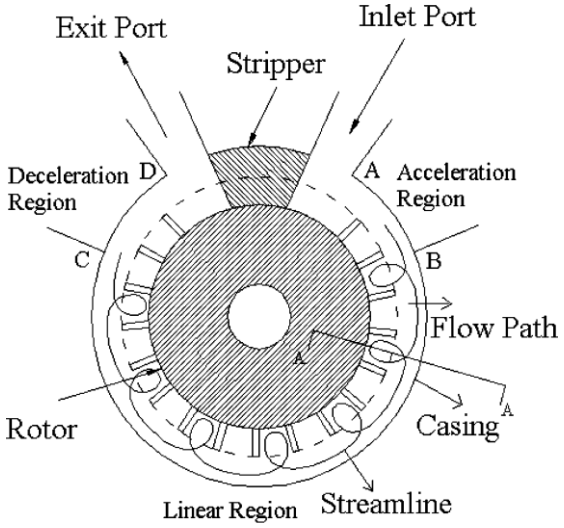

Fig.1 Spiral passage of flow pattern in RP [1]

The RP has desirable characteristic of continuous discharge flow regarding the high level of discharged pressure. Due to the wide applications of the RP, in irrigation and industry, their operation principles and methods of their performance enhancement were investigated during years using experimental tests, theoretical models, and recently computational fluid dynamics. Several literatures considered the fundamentals of the RP such as Shirinov and Oberbeck 2011 [2] and Raheel and Engeda 2002 [3], provided a detailed discussion on the fundamentals, working principle, and the useful applications of these pumps. They also discussed the main features of these type of pumps compared with those of other pumps and provided design studies using different numerical techniques (1-D and 3-D) as described by Quail et al. 2012 [4]. Despite these features, RP have low hydraulic efficiency ranging between 30% and 50%. Due to the drawbacks of these type of pumps, many researchers introduced various ways of design modifications methods to improve the performance of these pumps as reported by Kaelsen-Davies et al. 2016 [5]. Horiguchi et al. 2009 [6] performed experimental and numerical study to compare two different types of impellers: symmetric and asymmetric. They observed that the pressure of the symmetric impeller was about 2.5 times the asymmetric one. The most common suggested modifications in previous works were the changing of inclination or chevron angles of the blades. Figure 2 shows the side view of the pump casing where the inlet blade angle $\boldsymbol{\alpha}$ is called chevron angle the outlet blade angle $\boldsymbol{\beta}$ is called inclination angle.

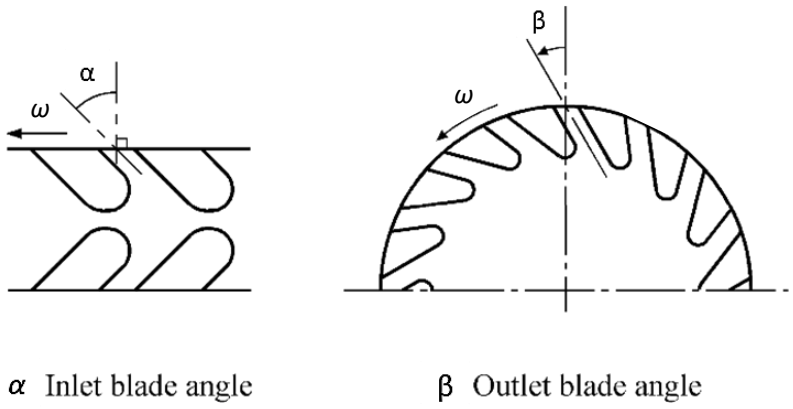

Fig. 2 Definition of the inlet blade angles (*chevron angle*) and outlet blade angles (*inclination angle*).

These modifications were done on each angle separately, which have crucial impacts on the head of RP as discussed by Horiguchi et al. 2009 [7], Teshome and Dribsa 2007 [8]. Nejad et al. 2017 [9] tested a symmetric impeller with three different values for the inclination angles +10°, +30° and +50°, it was observed that the head coefficient increased at inclination angles of +10° and +30° and decreased at angle of +50° compared with the radial blades. Horiguchi et al. 2009 [7] found that at inclination angle around +15° the maximum efficiency was achieved, this observation was also supported by Choi et al. 2013 [10], Nejadrajabali et al. 2016 [11] and Nejad et al. 2018 [12]. In similar way, Kanase et al. 2017 [13] changed the chevron blade angles of the regenerative pump, it was observed that the maximum efficiency occurred at chevron angles of 15° as well as concluded by Choi et al. 2013 [10]. Many researchers investigated experimentally and numerically the effect of modifying other geometrical parameters, like Fleder and Bohle 2015 [14], Rajmane et al. 2015 [15], Karanth et al. 2015 [16], Maity et al. 2015 [17], Isaev 2019 [18] and Li et al. 2020 [19].

Other researchers studied the effect of changing the number of blades (vanes) of the impeller on the performance of pump (Rajmane and Kallurkar 2015 [15]; Isaev 2019 [19]). It was concluded that increasing the number of blades, up to a certain number, increased the head of the pump. Whereas, further increase the blades number caused a blocking in flow, and consequently, decreased the performance of RP. The analysis of fluid flow in RP is not stopped

there, many researchers provided mathematical models and analysis for these types of pumps generally or for specific applications and they simply provided loss models without using empirical coefficients (Badami 1997 [20]; Song et al. 2003 [21]; Raheel and Engada 2005 [1]; Meakhail and Park 2005 [22] and Yoo et al. 2005-2006 [23, 24]). To the authors knowledge, no one in the literature reviewed, examined the impact of combination of simultaneous change of the inclination angle and chevron angle on the performance of REP. In the current work, this point is examined on an impeller with an inclination and chevron angles of +15° each and their effect on the discharged pressure is compared with that produced by the standard radial impeller. A model is built using CFD programs and is validated by comparing the numerical results with the experimental data of Horiguchi et al. 2009 [7].

2- The investigated Pump

In the current work, a numerical model is built and validated based on the results obtained by Horiguchi et al. 2009 [7]. The micro-RP considered has the same specifications and dimensions tabulated in Table 1 and illustrated in Figs. 3a and 3b.

Table 1 Dimensions of the pump used in the validation stage [7]

Position	Symbols	Description	Value	Unit
Casing	a_1	Depth of Channel	6	mm
	a_2	Height of Channel	15.5	mm
Clearance	c_1	Front/Rear Clearance	1.2	mm
	c_2	Side Clearance	5	mm
Impeller	α	Inlet Blade Angle	0	deg.
	β	Outlet Blade Angle	0	deg.
	b_1	Depth of Blade	8	mm
	b_2	Height of Blade	10.5	mm
	D_1	Diameter of the Hub	54	mm
	Z	Number of Vanes	16	[-]
	D_T	Diameter of the Tip	75	mm
	t_1	Thickness of Blades	5	mm

Data used in the present work are taken from reference [7]. The pump performance was determined by using a control valve at the discharge pipe to adjust the flow rate by measuring the volume of the discharged fluid. The suction and the discharge pressures were measured through pressure taps installed on the suction and the discharge pipes. The water at ambient temperature 25^{o}C was used as the working fluid. A motor with rotational speed of 600 rpm was used to drive the pump. The inlet and the outlet pipes included in the experimental setup are considered in the current numerical simulation.

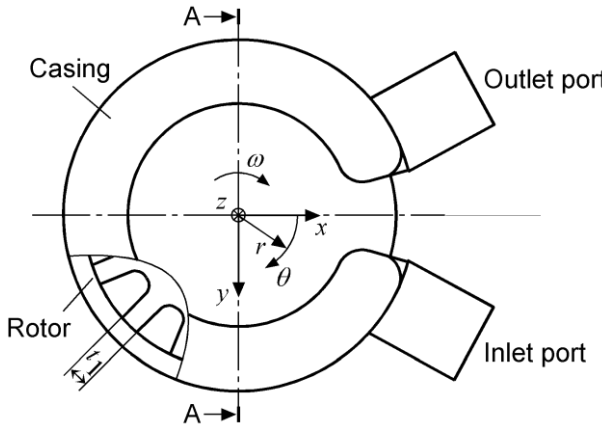

Fig. 3a Schematic diagram for the RP [7]

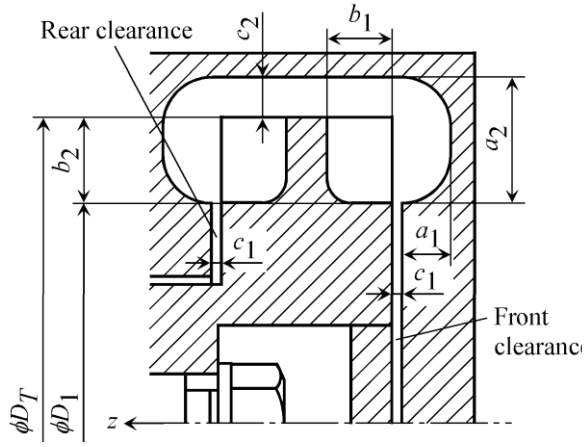

Fig. 3b Schematic diagram for the RP: View of A-A cross-section [7]

3- Numerical Approaches and Validations

In order to investigate the suggested modifications, a commercial software ANSYS CFX-19.0 is used to perform 3D unsteady simulation for the flow analysis of the described RP. The Reynolds Averaged Naiver-Stokes equation (RANS) combined with the Sheer Stress Transport (SST) turbulence model are employed, as recommended by [7]. The Reynolds number, defined based on the diameter of impeller D_T and the tip speed U_T, is about 2×10^5. To keep the fine meshes near-wall capable of resolving the viscous sub-layer, y^+ is kept in the range of 30~300 to comply with the log-law [25]. The computational domain is divided into three main parts as illustrated in Fig. 4a. The first one is the casing domain which contains the fluid flow around the impeller and surrounded by the external walls of casing body, the second and the third ones are the inlet pipe flow domain and the outlet pipe flow domain, respectively. In the casing flow part, the domain is divided into two parts as well, as shown in Fig. 4b; the dynamic layer domain, that represents the fluid layer rotating between walls of the impeller and fluid layer just above the impeller body; Fig. 5a and the static domain, which represents the remained part located between the casing body of the pump and the dynamic flow layer above the impeller, Fig. 5b.

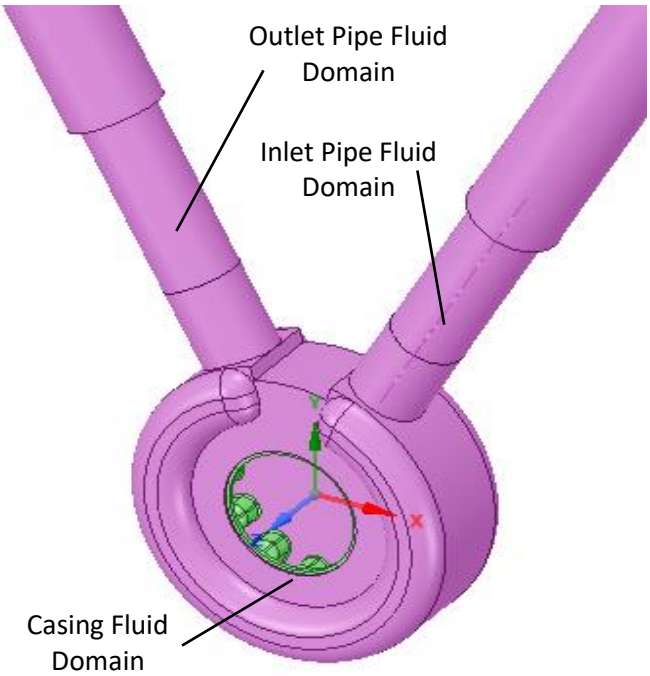

Fig. 4a Computational domain for RP

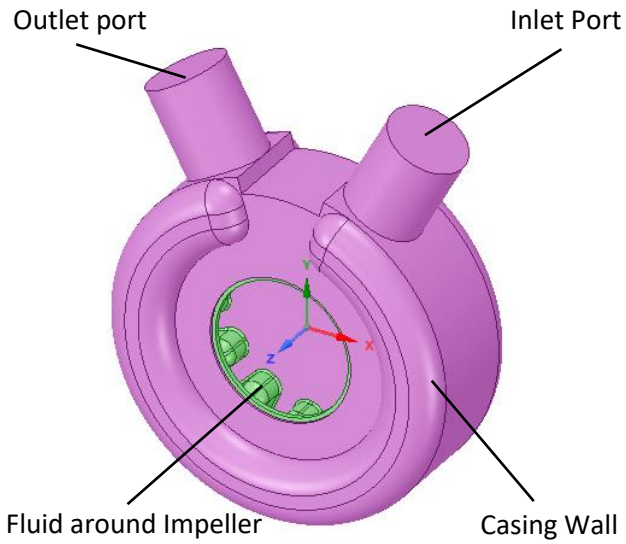

Fig. 4b Casing of RP

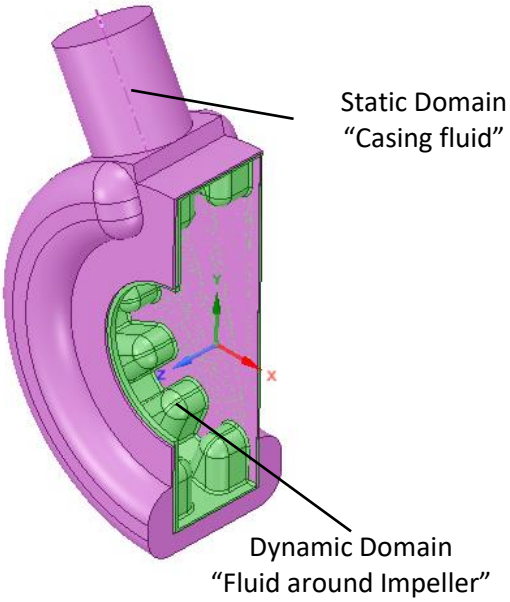

Fig. 5a Cross-section in the casing fluid domains

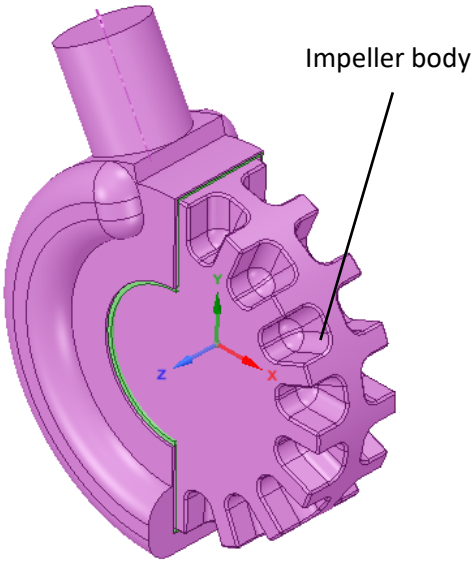

Fig. 5b Cross-section in the radial pump impeller

The lengths of the inlet and outlet pipes are about 11.1 and 13.5 times the casing diameter, respectively similar as in [7]. The centerline of the inlet pipe and outlet pipe are at angles of -28.6º and +28.6º from the Y-axis, respectively, as shown in Fig. 6.

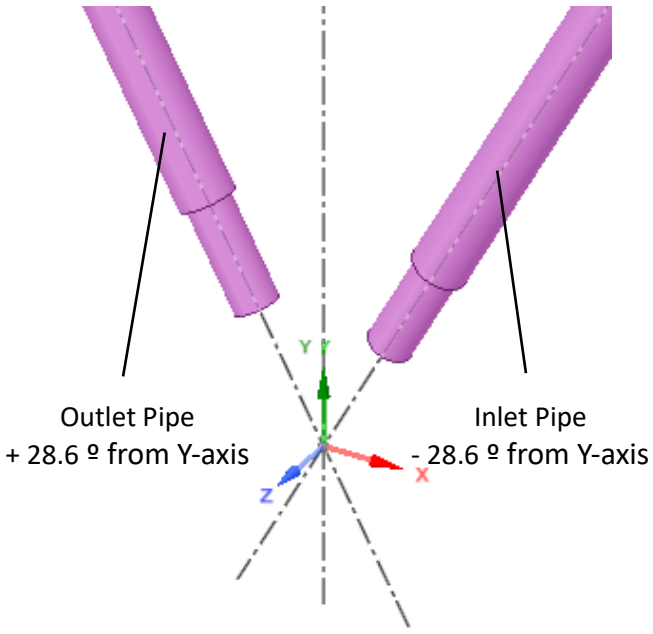

Fig. 6 Outlet and Inlet pipes

The Boundary conditions in these current simulations are similar to that employed in [7]:

- At inlet: the boundary set to be a constant static pressure and the flow is normally directed to the boundary condition with a medium turbulence intensity of 5%, which is a standard inflow boundary condition.
- At outlet: the boundary condition is set to the opening with variable pre-defined mass flow rate (0.0218, 0.05, 0.109, 0.1635, 0.218, 0.2725 and 0.3815 kg/s).
- The no-slip condition is employed near the solid walls.

The multi-zone meshing topology is used, where triangular prisms are employed near the walls and tetrahedral mesh elsewhere as shown in Figs 7, 8, 9 and 10.

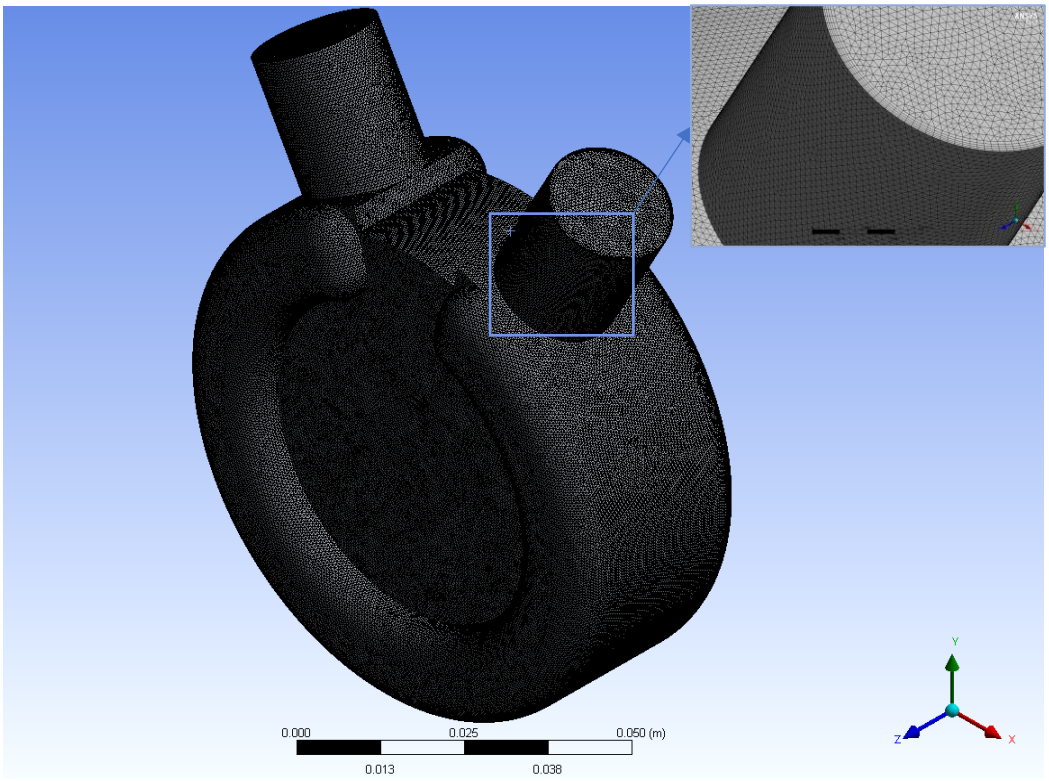

Fig. 7 Mesh topology for the static domain

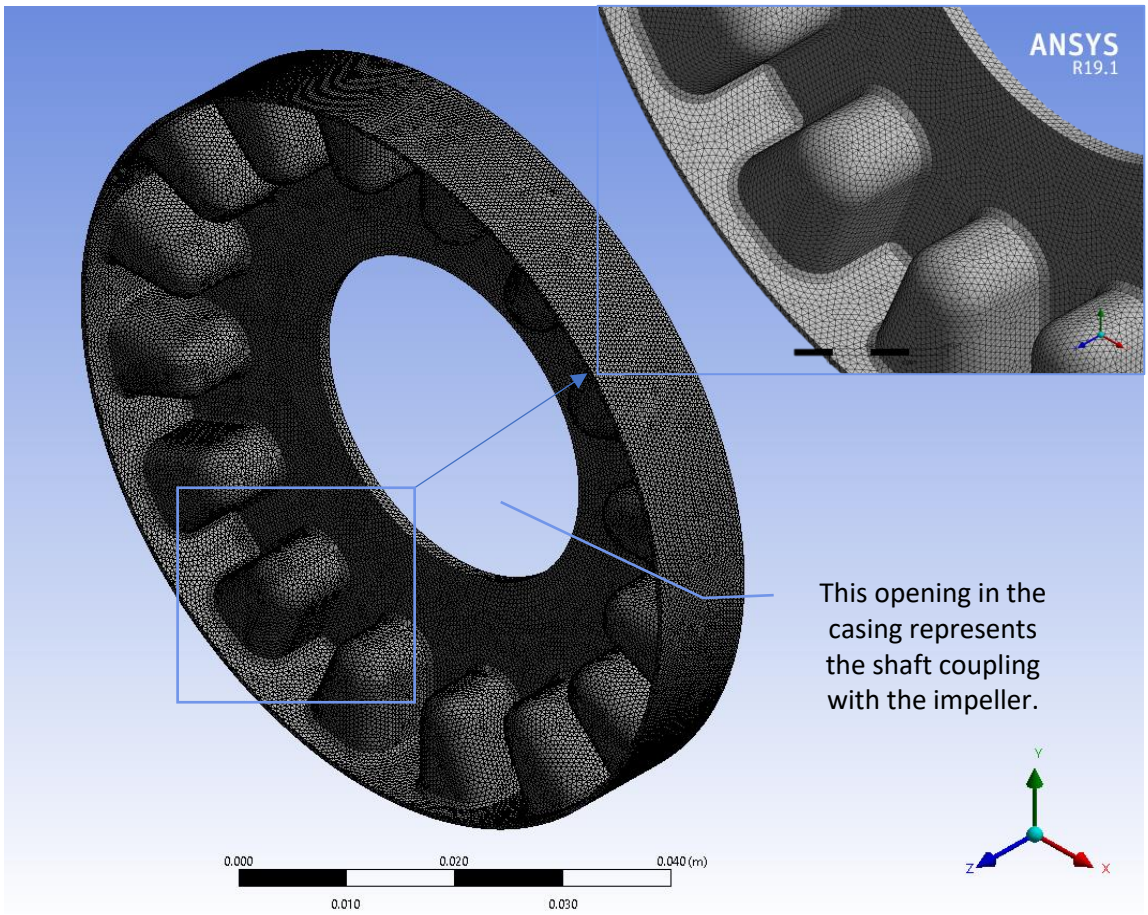

Fig. 8 Mesh topology for the dynamic domain: section view

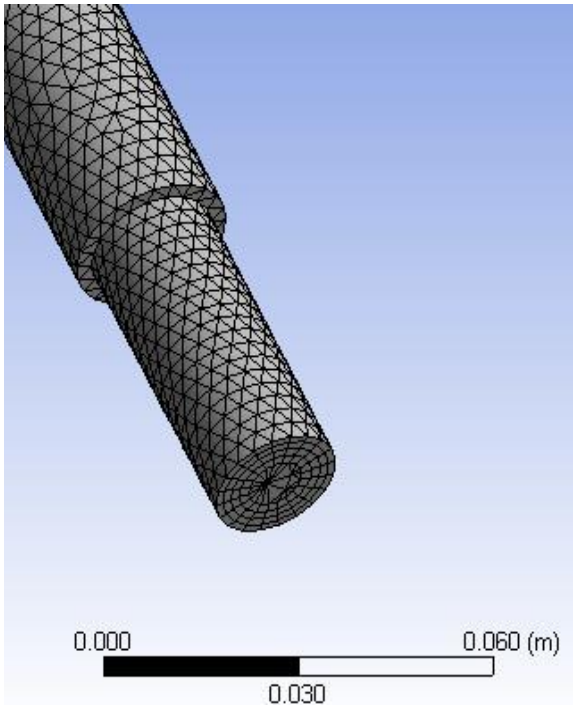

Fig. 9 Mesh topology for the outlet pipe

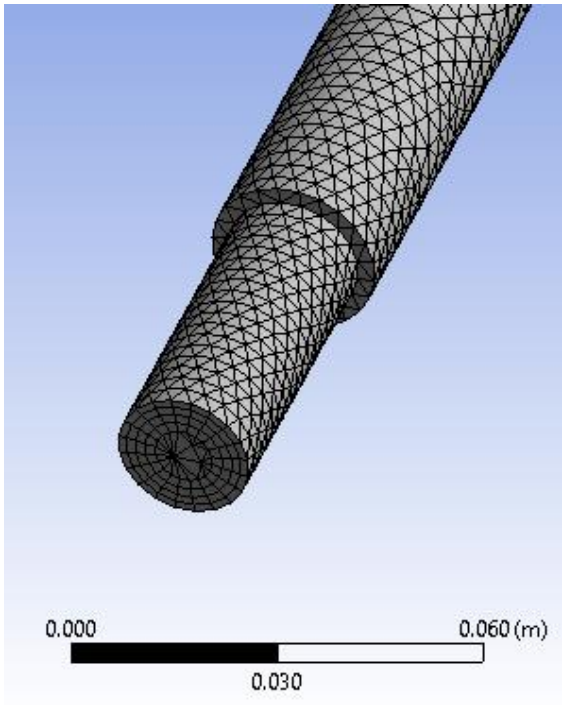

Fig. 10 Mesh topology for the inlet pipe

In order to achieve convergence conditions, The study of the mesh independency is held on a various number of mesh elements N of 0.2 million (M), 0.5M, 0.7M, 1.2M, 1.9M, 3.2M and 4.5M. Two variables are tested to examine the mesh independency, the flow coefficient $\emptyset$ and the head coefficient ψ. Where the flow coefficient $\emptyset$ is calculated from the flow rate Q passing through the pump and the cross-section area A_c = ($2a_1$ + $2b_1$ + $2c_1$ + t) a_2 - ($2b_1$ + t) of the channel (See Figs. 2 and 3),

$$\emptyset = \frac{Q}{A_c\, U_T}, \tag{1}$$

Where $U_T = \pi\, D_T\, \omega$ / 60 is the tip speed of impeller at rotational speed ω in revolutions per minute. The head (pressure) coefficient ψ is calculated as a function of flow density ρ, U_T, and the difference between the average values of pressures at discharge and suction sides ($\Delta P = P_d - P_s$) at walls of the pipe as follow,

$$\psi = \frac{\Delta P}{0.5\, \rho\, {U_T}^2}, \tag{2}$$

The head coefficient "ψ" is calculated and plotted at different number of mesh elements as shown in Fig. 11. It can be observed that the value ψ becomes independent on the grid size, when the mesh element reaches $N \geq$ 1.2M for different flow rates. As a consequence, and to save the computational resources, the simulations used for the analysis are discretized over N=1.2 M grid elements distributed as follows:

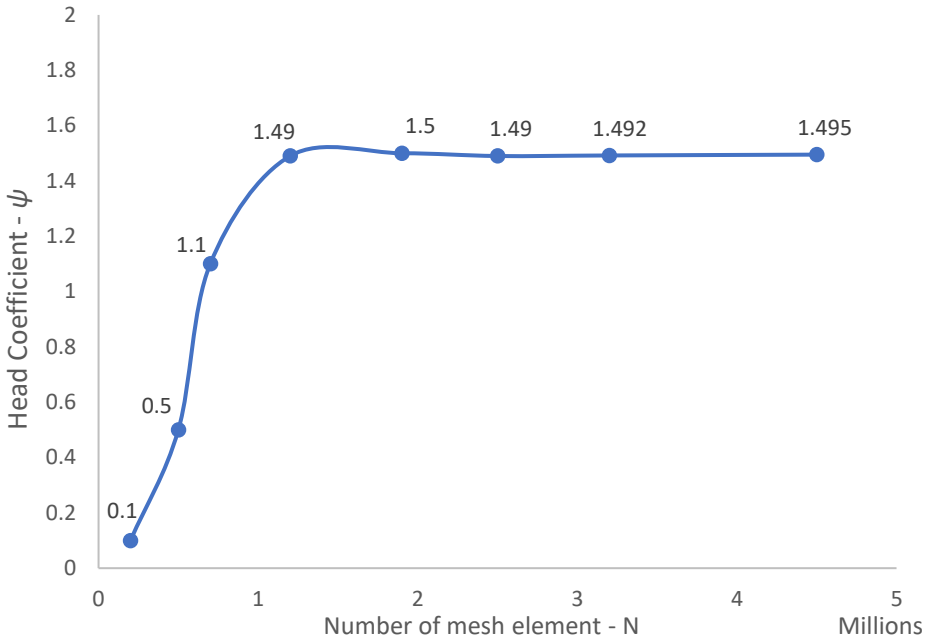

Fig. 11 Head coefficient "ψ" versus the number of mesh elements.

The meshes are distributed as following:

- 725,000 elements in the casing (static fluid domain) as shown in Figs. 7.
- 325,000 elements in the impeller (dynamic domain) as shown in Figs. 8.
- 70,000 elements in the inlet pipe (Fig. 9).
- 80,000 elements in the outlet pipes (Fig. 10).

In these simulations, the impeller is rotated in three complete revolutions with a total duration time of 0.3 second (unsteady simulation). The setting of the interface surfaces model between impeller and the side flow channel is set to be transient "rotor-stator", due to the change of the relative position between the impeller and the side channel at each time step. For time integration, the second-order backward Euler is kept in the transient scheme. Figure 12 shows comparisons between the current simulation and the experimental and numerical results introduced by Horiguchi et al. 2009 [7]. It can be concluded that, the current flow simulation shows an excellent agreement with the experimental and computed data of Horiguchi et al. 2009 [7].

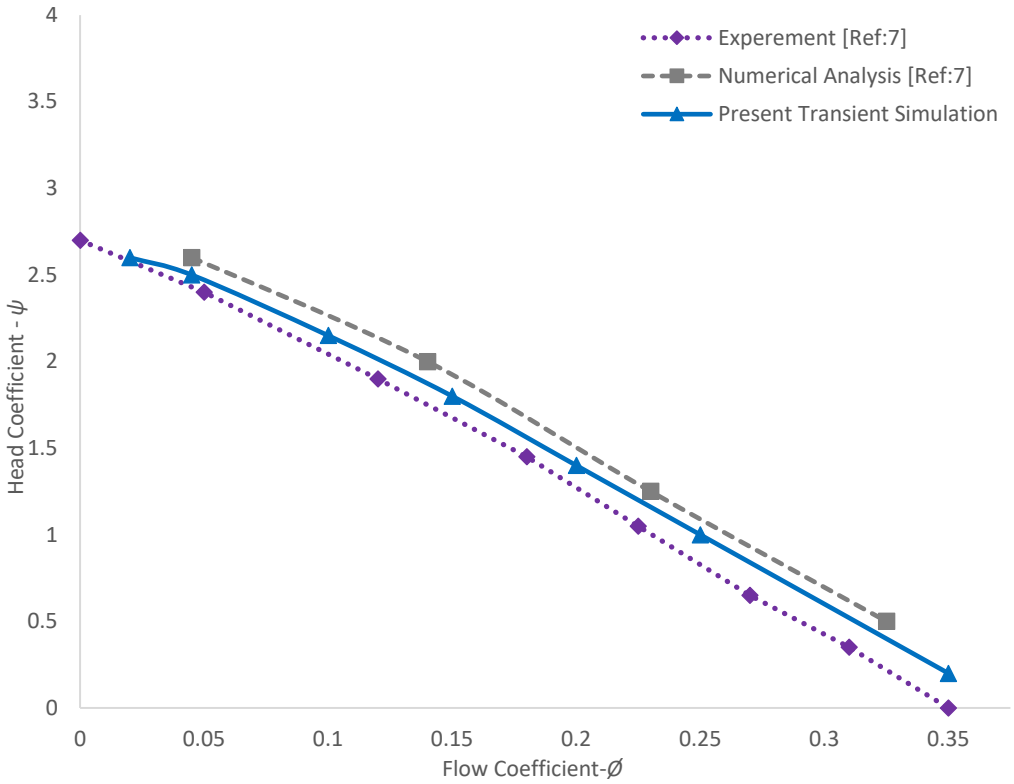

Fig.12 Flow coefficient versus head coefficient of the RP: comparison between the present transient simulations of the current work with that of the experimental and numerical works done by Ref. [7].

4- Suggested Geometrical Modifications

The head of the RP was found increased by changing and optimizing the inclination and chevron blade angles. Several researchers as Nejad et al. 2017 [9], Horiguchi et al. 2009 [6, 7] and Kanase et al. 2017 [13] performed geometrical modification on the radial impeller of the RP shown in (Fig. 13) by changing either their inclination angels or chevron angles separately with an angle of +15^{o} .

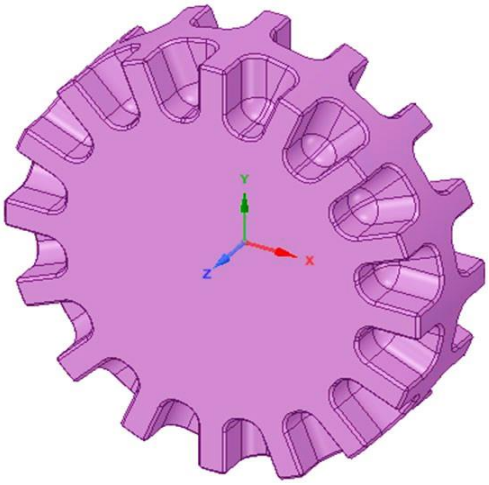

Fig.13 Standard blade impeller (RB).

Therefore, in the present study it is suggested to apply a suitable combination of geometrical modification for both angles (inclination and chevron) simultaneously. A selected value of

+15° is used for both angles. This suggested combination will be applied as double forward blade impeller (DFB) as it is shown in Fig. 14a, 14b and 14c.

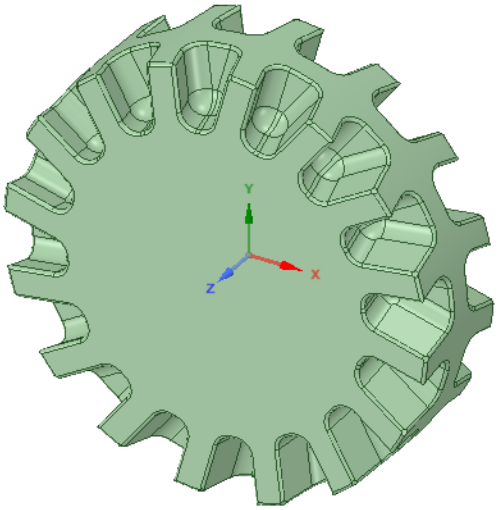

Fig.14a DFB impeller: 3D view

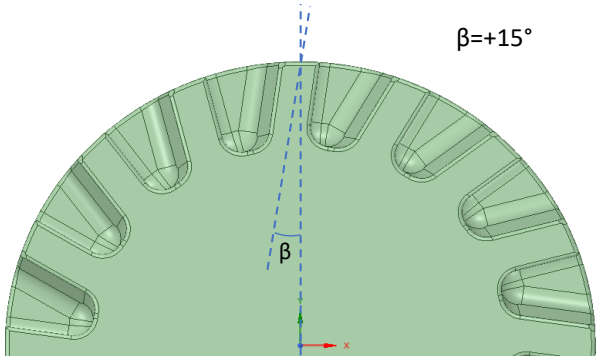

Fig.14b DFB impeller: Outlet blades angle view

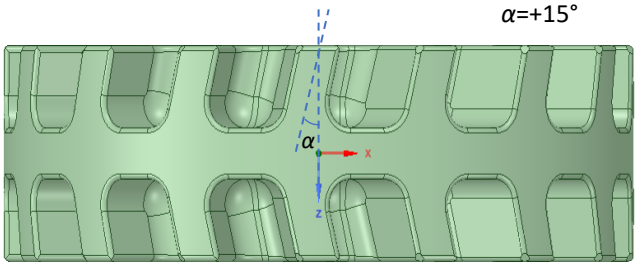

Fig.14c DFB impeller: Inlet blades angle view

5- Results and Discussions

The results obtained from the suggested modifications will be discussed in details by comparing the pressure delivered from the modified impeller, DFB, with that from the standard one, RB. The pressure contours are plotted in each case at 5 mm apart from X-Y plane towards the positive direction of Z-axis.

5-1 Effect of double forward angle modification on the performance of regenerative impeller

The suggested modification applied is the double forward impeller, DFB, with chevron angle α=+15^o and inclination angle β=+15^o (see Fig. 14). Figures 15 and 16 show the 2D color contours of pressure of the flow fields for the standard case with radial angles, RB, and a case with double forward angles, DFB, respectively. It can be observed that the suggested modification increases the range of discharged pressure (pressure coefficient), about 50% more than that discharged from the simple radial impeller (standard one).

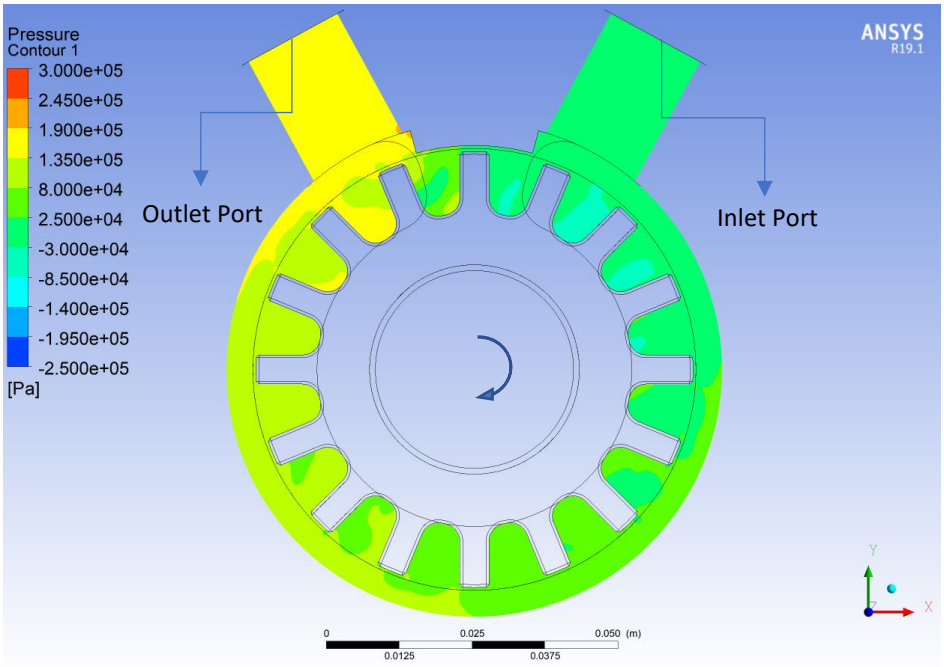

Fig. 15 Radial blades impeller (pressure contour at +5 mm along +Z-axis)

.

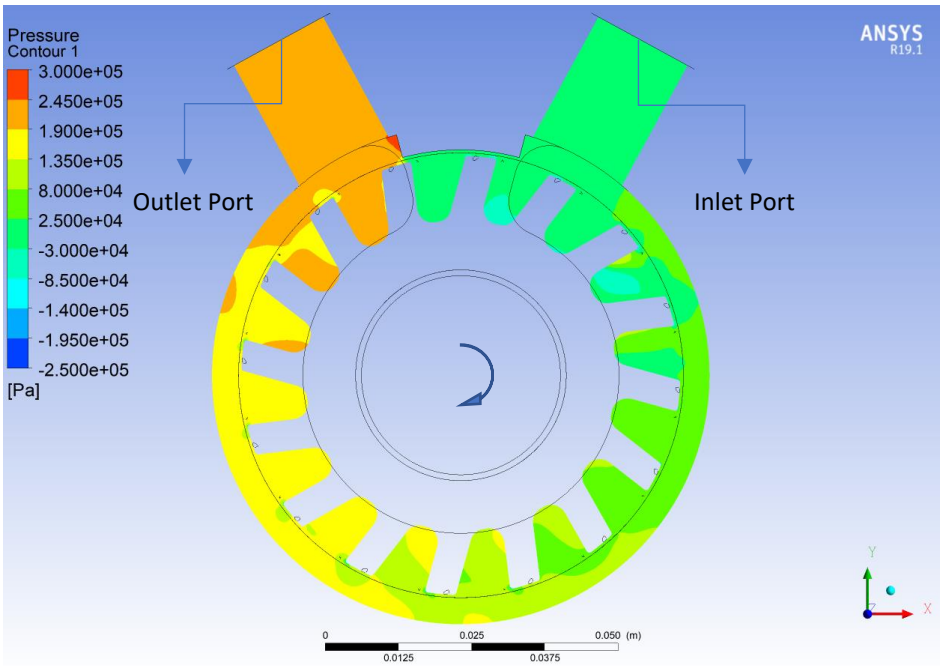

Fig. 16 Double forward blades impeller (pressure contour at +5 mm along +Z-axis)

.

5-2 Assessment of the suggested modifications

By comparing, both Figs 15 and 16, it can be observed that the pressure of the flow field around the blades in case of double forward blade modification, DFB, is larger than that of the radial blade, RB. Figures 17 shows the instantaneous discharge flow pressure at the outlet pipe ports after three complete revolutions of impeller for both cases: radial blades and double forward blades.

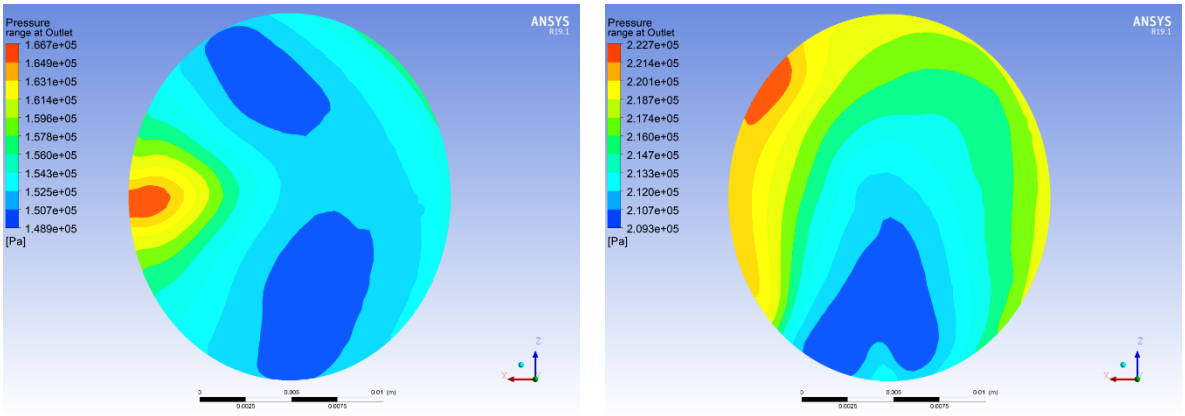

Radial Blade (RB) Double Forward Blade (DFB)

Fig. 17 Instantaneous discharged pressure range from the casing outlet of the RB and DFB

It is also observed from Fig. 17 that the discharged local pressure range for the double forward blade, DFB, is higher than the standard radial impeller, RB. This means that the DFB produces largest discharge pressure compared with that of RB one. This result can be also be concluded from tracking the pressure developing between each blade of the double forward, DFB, and the radial blades, RB, through a flow path located +5 mm from the X-Y plan. Figure 18 shows the velocity vectors and the direction of the flow at the tracked path for the radial pump. The tracked flow path for the double forward pump is done with the same criteria of the radial one.

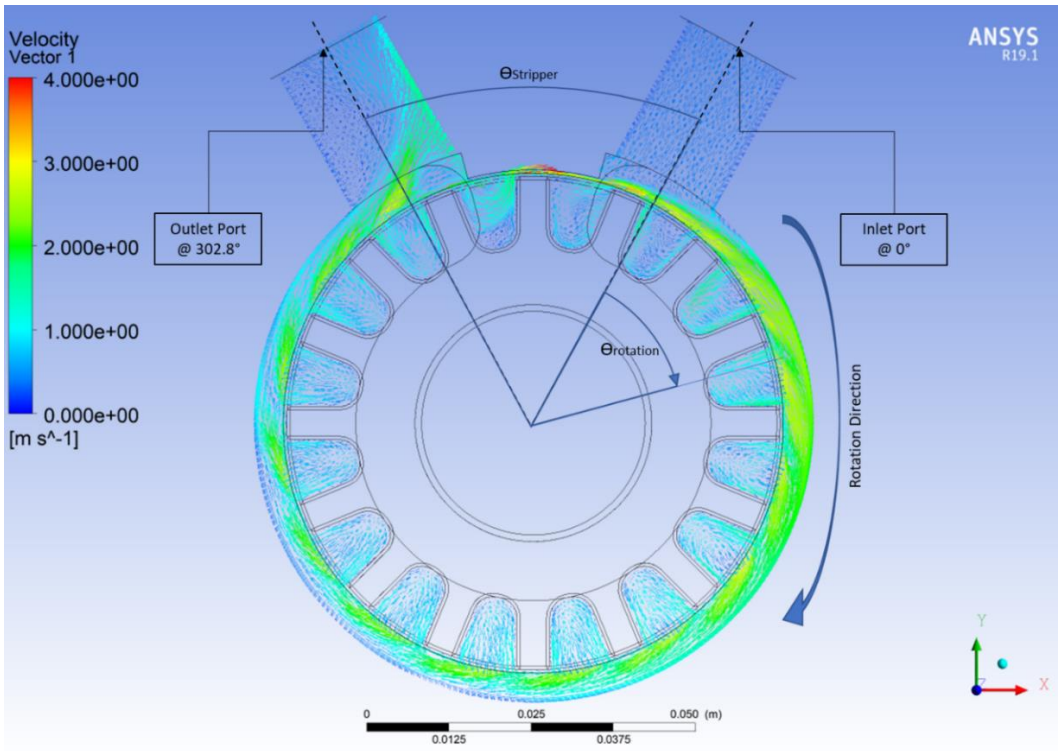

Fig. 18 Velocity vector of radial blades impeller RB with showing the flow path direction in a certain plane.

The pressure tracking across this flow path is presented in Fig. 19 showing the evidence of local pressure variation between each blade of impeller for the two investigated cases. Moreover, it can be observed that the local pressure in case of the double forward impeller is greater than that in the radial impellers case for all angles "from Y-Axis" greater than 60.

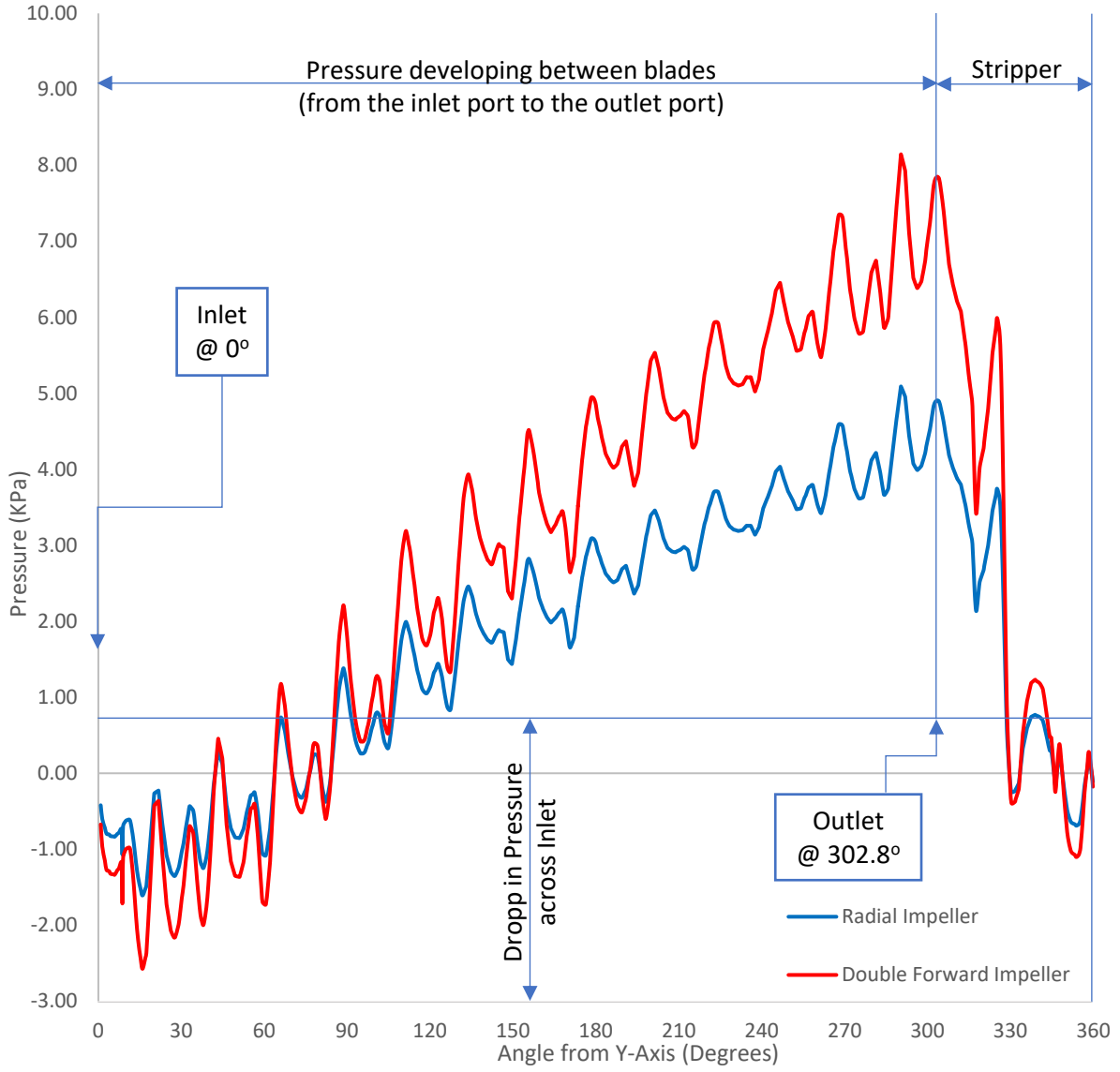

Fig. 19 Pressure variation along fluid path angle for the RB and DFB impellers.

In order to quantify the performance of the pumps, the pressure (head) coefficient ψ (Eq. 1), pump efficiency η and torque coefficient τ, are considered,

$$\eta = \frac{\psi.\emptyset}{2.\tau} \quad , \tag{3}$$

where the torque coefficient τ is calculated as a function of the torque T generated by the impeller blades on the fluid flow through the pump and rotational speed ω,

$$\tau = \frac{T.\omega}{\rho.A_c.{U_T}^3} \quad . \tag{4}$$

Figure 20 shows the head coefficient versus the flow coefficient (ψ-$\emptyset$) and efficiency versus the flow coefficient (η-$\emptyset$) for the simple radial impeller RB, and the double forward impeller,

DFB. It is found that the pressure coefficient and pump efficiency of double forward angle case are greater than those of the standard radial impeller.

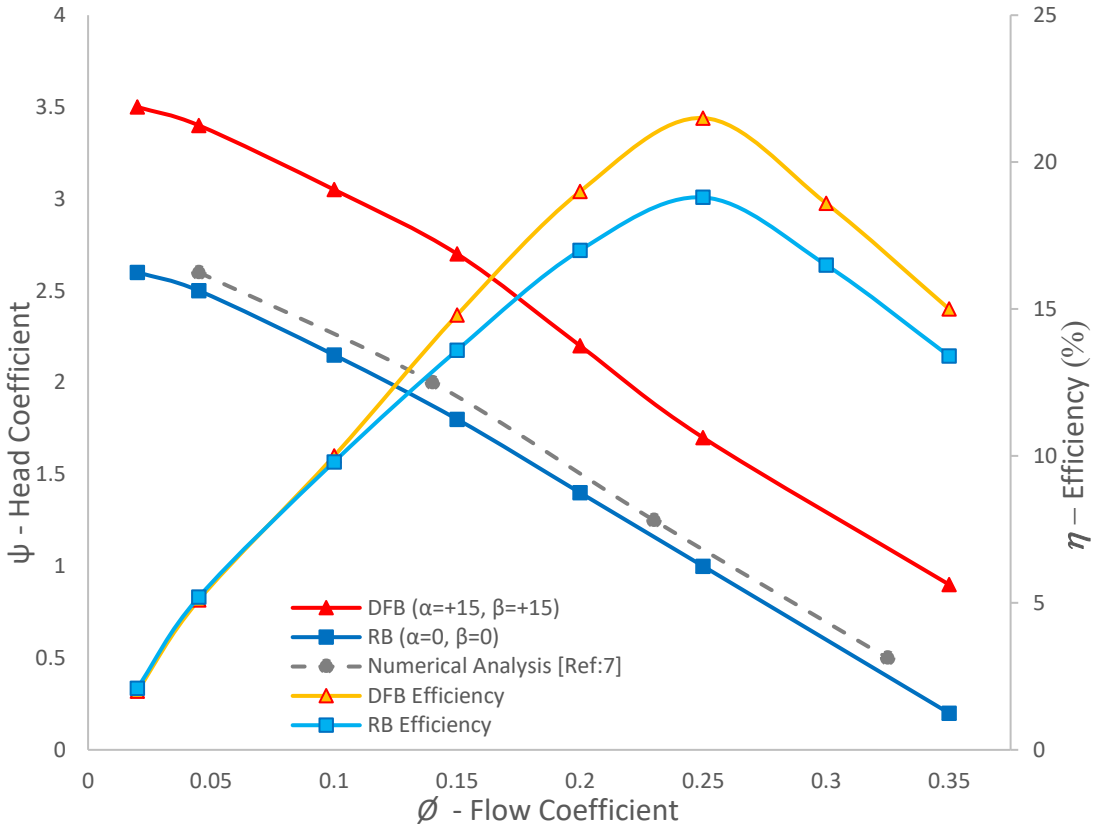

Fig. 20 Head Coefficient and Efficiency versus flow coefficient graph for the double forward impeller comparing with the simple radial one.

It is observed from Fig. 20 that at the flow coefficient around 0.25, the design condition, the percentage of improvement in the pump head is 70% in case of the double forward impeller compared to the standard radial impeller. As the flow coefficient decreases, the percentage of improvement of the pump head of DFB is decreases and tends to 40% larger than the standard radial impeller. Also, the percentage of efficiency improvement in DFB case is highlighted at the design condition (flow coefficient around 0.25) and reaches 14%higher than the standard radial impeller.

5-3 **Double angle modifications versus single one**

In this section, the pump performance in the present case with simultaneous change of the two angles (referred as a double modification) is compared to the cases interpreted by many researches where the change is confined to one angle, while keeping the other unchanged (referred as a single modification) as suggested previously by many researches, (Nejad et al. 2017 [9]; Horiguchi et al. 2009 [7]; Nejadrajabali et al. 2016 [11]). In total, four cases are investigated and compared with the radial standard impeller in Fig. 21: (1) DFB (α=+15, β=+15), (2) RB (α=0, β=0), (3) changing the inclination angle only, **SFI** (α=0, β=+15), and (4) changing the chevron angle only, **SFC** (α=+15, β=0). It is obvious that the double forward modification, DFB, (α=+15, β=+15) is the best among all the cases. The improvement is among 70% in head pump at the max. efficiency point.

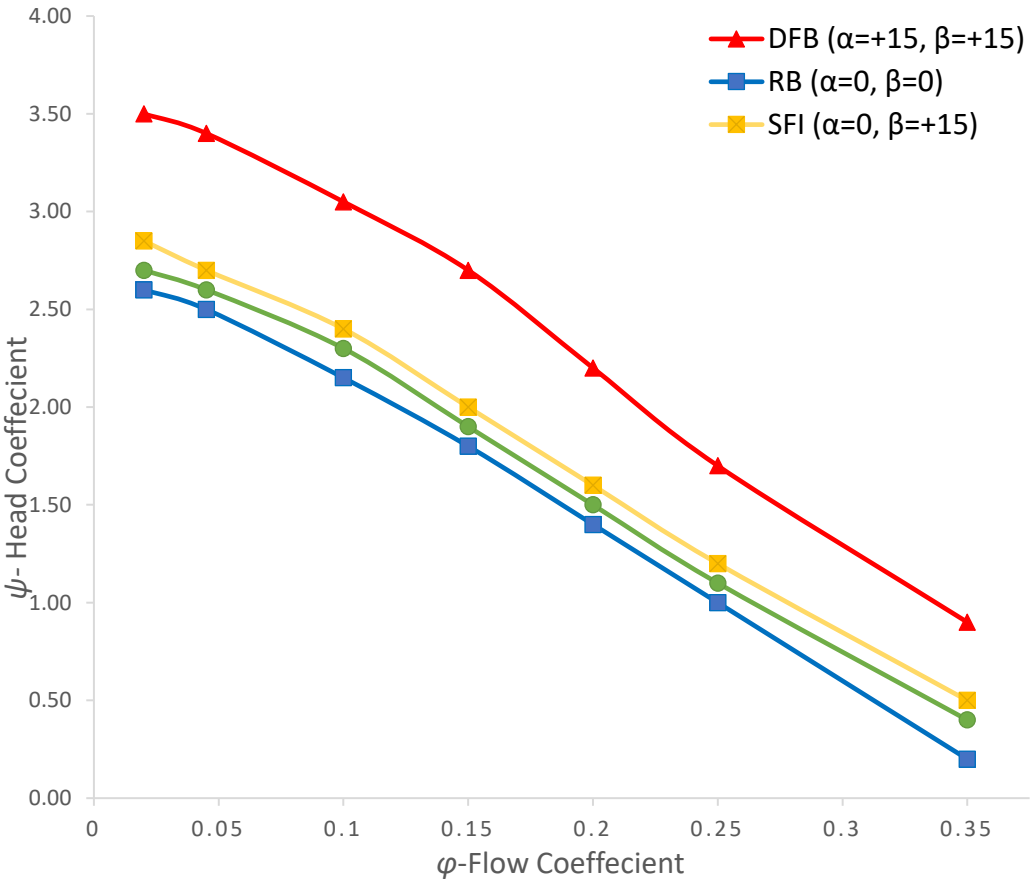

Fig. 21 Head coefficient versus flow coefficient for various types of angle modifications compared with the RB impeller.

6- Conclusion and Discussion

A computational simulation is performed to improve the performance of the RP. First the employed models are validated with available published numerical and experimental results. The improvement due to blade design suggestion is obtained by changing two important angles: inclination and chevron blade angles simultaneously. It has been found that the changing of both angles at the same time has a significant impact on the pumps performance which can be summarized as follows:

1- A higher pressure (head) coefficient of the regenerative pump is obtained by changing the standard radial impeller angles (α= 0^o and β= 0^o) to chevron angle α=+ 15^o and inclination angle β= +15^o.
2- The improvement in pressure coefficient of the RP can be obtained by using an impeller with double forward blade of chevron angle α=+15^o and inclination angle β= +15^o reaching 70%, at the design condition, compared with the simple radial impeller (α= 0^o and β= 0^o) at the same value of the flow rate.
3- The pump efficiency at the design flow rate condition is increased by 14% in case of double forward case compared to the standard radial impeller.
4- The double forward blade improvement is much higher than that obtained by the single forward blade for each angle.

7- References

1 Raheel, M.M. and Engeda, A. Systematic design approach for radial blade regenerative turbomachines. J. Propul, Power, 2005; 21(5):884-892.

2 Shirinov, A., and Oberbeck, S. High vacuum side channel pump working against atmosphere. Vacuum, Elsevier, 2011; 85:1174–1177.

3 Raheel, M. and Engeda, A. Current status, design and performance trends for the regenerative flow compressors and pumps. ASME IMECE, 2002; 99-110: 39594.

4 Quail, F.J., Scanlon, T., and Baumgartner, A. Design study of a regenerative pump using one-dimensional and three-dimensional numerical techniques. Eur. J. MechB/Fluids, 2012; 31: 181–187.

5 Karlsen-Davies, N.D., and Aggidis, G.A. Regenerative liquid ring pumps review and advances on design and performance. Appl Energy, 2016; 164: 815–825.

6 Horiguchi, H., Matsumoto, S., Tsujimoto, Y., Sakagami, M., and Tanaka, S. Effect of internal flow in symmetric and asymmetric micro regenerative pump impellers on their pressure performance. Int. J. Fluid Mach. Syst., 2009; 2 (1), 72-79.

7 Horiguchi, H., Wakiya, K., Tsujimoto, Y., Sakagami, M., and Tanaka, S. Study for the increase of micro regenerative pump head. Int, J. Fluid Mach. Syst., 2009; 2(3), 189-196.

8 Teshome, Y., and Dribsa, E. CFD study of the performance of regenerative flow pump (RFP) with aerodynamic blade geometry. MS Thesis, University of Addis Ababa, Ethiopia, 2007.

9 Nejad, J., Riasi, A., and Nourbakhsh, A. Parametric study and performance improvement of regenerative flow pump considering the modification in blade and casing geometry. Int. J. Numer. Methods Heat Fluid Flow, 2017; 27(8): 1887–1906.

10 Choi, W.C., Yoo, I.S., and Park, M.R. Experimental study on the effect of blade angle on regenerative pump performance. Proc IMechE Part A: J. Power and Energy 2013; 227: 585–592.

11 Nejadrajabali, J., Riasi, A., and Nourbakhsh, S.A. Flow pattern analysis and performance improvement of regenerative flow pump using blade geometry modification. Int. J. Rot. Mach., 2016; (77): 1-16.

12 Nejad, J., Riasi, A., and Nourbakhsh, S.A. Efficiency improvement of regenerative pump using blade profile modification: experimental study. Proc IMechE, 2018; 2018: 1-8.

13 Kanase, R.S., Kasturi, M.L., Pise, A.T. and Garje, P.C. Experimental and CFD analysis of regenerative pump. ISHMT-ASTFE, 2017; 3(4), 1135-1141.

14 Fleder, A. and Bohle, M. A systematical study of the influence of blade length, blade width, and side channel height on the performance of a side channel pump. ASME J. Fluids Eng. 2015; 137(12), 121102.

15 Rajmane, S.M. and Kallurkar, S.P. CFD analysis of domestic centrifugal pump for performance enhancement. IRJET, 2015; 2(2), e-ISSN: 2395-0056, p-ISSN: 2395-0072.

16 Karanth, V.K., Manjunath M.S., Kumar, S., and Sharma, N.Y. Numerical study of a self-priming regenerative pump for improved performance using geometric modifications, IJCET, 2015; 5(1), pp.104–109.

17 Maity, A., Chandrashekharan, V. and Afzal, M.W. Experimental and numerical investigation of regenerative centrifugal pump using CFD for performance enhancement. Int. J. Curr, Eng, Technol, 2015; 5: 2898–2903.

18 Isaev, N., The effect of design parameters of the closed type regenerative pump the energy characteristics, IOP Conf. Series: Materials Science and Eng., 2019.

19 Li, Q.Q., Zhao, G.S., Wu, C.S., Wu, P., Wu, D.Z., and Guo, C.L. Investigation on the energy exchange characteristics of the regenerative flow pump in an automobile fuel system. J. Fluid Eng., 2020; 1(142), 111206.

20 Badami, M. Theoretical and experimental analysis of traditional and new periphery pumps. SAE Technical paper Series, 1997; 971074: 45–55.

21 Song, J.W., Engeda, A., and Chung, M.K. A modified theory for the flow mechanism in a regenerative flow pump. Proc IMechE, Part A: J. Power and Energy 2003; 217:311–321.

22 Meakhail, T. and Park, S.O., An improved theory for regenerative pump performance. Proc IMechE, 2005; 213-222.

23 Yoo, I.S., Park, M.R. and Chung, M.K. Improved momentum exchange theory for incompressible regenerative turbomachines. Proc IMechE, Part A: J Power and Energy 2005; 219: 567–581.

24 Yoo, I.S., Park, M.R., and Chung, M.K. Hydraulic design of a regenerative flow pump for an artificial heart pump. Proc IMechE, Part A: J Power and Energy 2006; 220: 699–706.

25 Versteeg, H.K. and Malalasekera W. An introduction to computational fluid dynamics: the finite volume method. Harlow, England: Prentice-Hall; 2007; 2, 57-60.